

RESIDUAL STRESSES DURING LIQUID MOULDING OF COMPOSITES USING HIGHLY REACTIVE THERMOSETS.

L. Barcenas^{1,2}, S. Sarojini Narayana^{1,2}, and P. Hubert^{1,2*}.

¹Structures and Composite Materials Laboratory, McGill University, Montréal, Canada.

²Centre de recherche sur les systèmes polymères et composites à haute performance (CREPEC).

* Corresponding author (pascal.hubert@mcgill.ca)

Keywords: Liquid moulding, highly reactive thermosets, residual stresses, process simulation

ABSTRACT

This manuscript aims to implement an integrated simulation strategy for the prediction of residual stresses and the final shape of composites with highly reactive thermoset matrix. The materials used for this analysis are Gurit prime 130 standard resin, and E-glass non-crimp fabric TG-15-N. An extensive experimental characterization work was performed to generate the fundamental material models for the resin cure kinetics, the cure shrinkage, the coefficient of thermal expansion and the resin viscoelastic modulus. Flow injection simulations were performed using PAM-RTM. The degree of cure evolution during injection was used as an initial condition for the simulation of curing and residual stresses using Abaqus COMPRO. The influence of the degree of cure evolution during injection was analyzed and compared with experimental results obtained from the manufacturing of a representative geometry.

1 INTRODUCTION

The transportation industry's interest in highly reactive thermosets stems from the potential to boost composite material production rates [1]. The use of highly reactive thermosets creates manufacturing and quality challenges for moulded parts, part design, and tooling. Dimensional distortion of composite materials parts is an inherent response of the residual stresses generated during the processing. The final shape of the composites depends on non-uniform resin flow, tooling effects, shrinkage, and cure gradients. Degree of cure gradients are more extensive with highly reactive thermosets during the filling stage [2]. These gradients produce a non-uniform spatial evolution of the mechanical properties of the composite, which has been shown to influence the prediction of the final shape of the composite [3].

Equation 1 shows the integral form of the stresses on the resin during processing [4]. The stresses are calculated from the evolution of the resin modulus, which is a function of time (t), the temperature (T), the degree of cure (α), and the time of applied strains defined as total time minus time of load application (t- τ). The strain (ϵ) comes from the cure shrinkage and the coefficient of thermal expansion, which both are dependent on the degree of cure.

$$\sigma(t) = \int_0^t E(t-\tau, T, \alpha) \frac{d\epsilon}{d\tau} d\tau \quad (1)$$

Equation 2 defines the sources of strains during the processing from chemical shrinking and thermal expansion where (V) is the volume.

$$\frac{d\epsilon}{d\tau} = \left(\frac{1}{V} \frac{dV}{d\alpha} \frac{d\alpha}{d\tau} \right)_{\text{Chemical Shrinkage}} + \left(\frac{1}{V} \frac{dV}{dT} \frac{dT}{d\tau} \right)_{\text{Thermal Expansion}} \quad (2)$$

This manuscript focuses on the study of the resin properties that are relevant for the development of residual stresses during the curing process. Constitutive models are used to describe the cure kinetics,

chemical shrinkage, thermal expansion, and viscoelasticity of the thermoset [3]. By incorporating these constitutive material models, the manuscript aims to provide a comprehensive understanding of how the material properties contribute to the development of residual stresses during the cure of highly reactive thermosets. These models can be valuable in optimizing the curing process parameters and predicting the resulting material behaviour, allowing the production of high-quality composite parts with controlled residual stresses.

2 MATERIALS

The preform used for this analysis is a Texonic TG-15-N NCS E-Glass with an areal weight of 518 g/m². The E-Glass material properties such as density, elastic modulus, specific heat, coefficient of thermal expansion and thermal conductivity were taken from COMPRO database [5-9]. The preform permeability was obtained from the work reported in [2]. The mould was assumed to have the material properties of Aluminum 6060 which include density, elastic modulus, Poisson's ratio, specific heat, coefficient of thermal expansion and thermal conductivity.

Gurit prime 130 standard resin system was analysed. This fast-curing matrix was characterized using a differential scanning calorimeter for the cure kinetics and glass transition [10,11]. A thermomechanical analyser was used for the coefficient of thermal expansion [4]. A rheometer was used to define cure shrinkage model [12]. Finally, a dynamic mechanical analyser was used for the elastic modulus characterization. These material properties were reported by [3]. A viscosity characterization work for this resin system was reported by [2]. The simulation assumed a rule of mixtures for the calculation of the composite material properties [13].

2.1 Thermo-viscoelastic Modulus

The generalized Maxwell model was used to account for the viscoelastic effects of the resin. Equation 3 shows the adapted equation for storage modulus (E') [4, 14-21]. This viscoelastic modulus model accounts for frequency, temperature, and degree of cure effects.

$$E'(\omega, T, \alpha) = E^r(\alpha, T) + [E^u(T) - E^r(\alpha, T)] \sum g_i [\omega^2 a_{T, \alpha}^2 \tau_i^2 / (1 + \omega^2 a_{T, \alpha}^2 \tau_i^2)] \quad (3)$$

where E^r is the relaxed elastic modulus with a dependency on degree of cure and temperature. E^u is the unrelaxed elastic modulus which has dependency on the temperature. A superposition horizontal shift factor $a_{T, \alpha}$ was used to account for the time-temperature superposition. The viscoelastic function Equation 3 is adjusted with the weight factors g_i for selected relaxation times τ_i (Table 1), where ω is the angular velocity defined by the frequency. Figure 1 shows the comparison of the experimental measurements with the thermo-viscoelastic model.

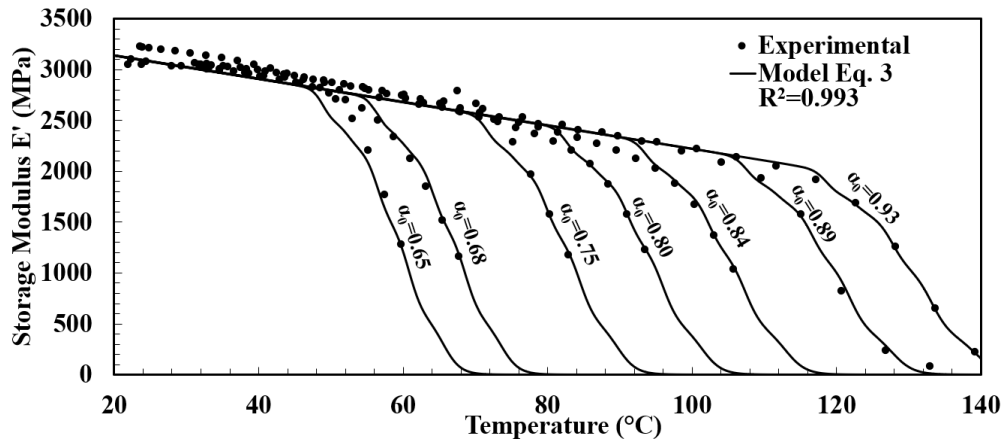


Figure 1: Experimental tests for coupons at different initial degree of cure compared with the thermo-viscoelastic model (Equation 3).

Table 1: Relaxation times and weight factors for the thermo-viscoelastic model Equation 3.

i	τ_i	g_i
1	1.0 E+00	0.1129
2	1.0E+01	0.0808
3	1.0E+02	0.2586
4	1.0E+03	0.3452
5	1.0E+04	0.2006

3 PROCESS MODELLING

The process simulation consisted of the integration of PAM-RTM software for the injection stage (filling simulation), and Abaqus-COMPRO software for the cure cycle and cool down (stress-deformation simulation). A single curvature plate of width 124 mm and radius 247 mm was designed for this analysis. A seven TG-15-N plies 3 mm thick laminate was considered giving a volume fraction of 0.47. Figure 2 shows the dimensions of the geometry used for the simulation and experimental validation.

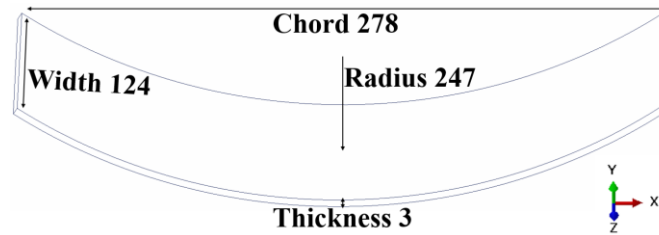


Figure 2: Geometry of the composite part. Dimensions in mm. $[0^\circ]_7$ layup with 0.47 volume fraction.

PAM-RTM software was used for the simulation of the filling during a heated resin transfer moulding. This software uses the finite volume analysis to solve Darcy's law. The permeability of preform and the resin viscosity (Section 2) were implemented in the flow simulations. Figure 3 shows the boundary conditions used for the filling simulation, where vacuum was applied on one side, and the resin at room (25 °C) temperature was injected on the opposite side with constant injection pressure ($P_{injection}$).

The external surfaces were set to have a constant mould temperature of 80°C ($T_{process}$). The injection pressure was varied as defined in Table 2. A minimal injection of 1.6 bar was required to fully impregnate the composite before the resin reached the gel point. Figure 3 shows the result of the degree of cure after an injection at 1.6 bar. Table 2 shows the filling simulation results performed on PAM-RTM with the variation of pressure and maximum degree of cure reached at the end of the injection (α_{max}). As the pressure is increased, α_{max} decreases. A reference case was added where a uniform low degree of cure ($\alpha=0.01$) was assumed. This can be achieved experimentally by pre-impregnating the preform, then the pre-impregnated layout is placed into the mould, which is at room temperature, finally the mould temperature is increased to 80°C.

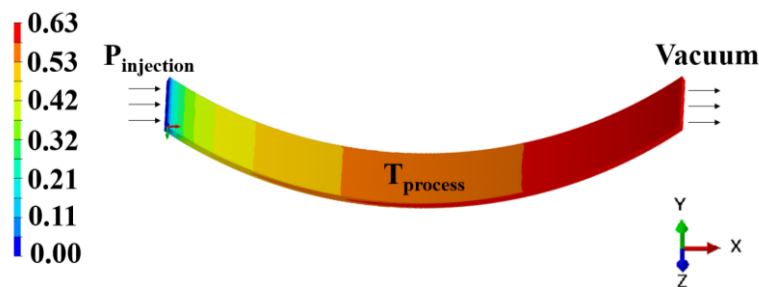


Figure 3: PAM-RTM result. Degree of cure variation in the part after full impregnation.

Table 2: Filling simulation results from PAM-RTM.

Case	Injection pressure (bar)	Mould temperature during injection ($^{\circ}\text{C}$)	Filling time (s)	α_{\max}
A	Reference	25	-	0.01
B	4.5	80	62	0.10
C	2.7	80	124	0.21
D	2.3	80	170	0.28
E	1.8	80	273	0.40
F	1.6	80	565	0.63

The stress-deformation simulation was computed using Abaqus-COMPRO following two steps. Figure 4 (a) shows the thermal and mechanical boundary conditions for the curing phase. An investigation of scaling has indicated that the out-of-plane convection of the mould with the environment is insignificant and frequently overlooked because the thickness of the composite is small in comparison to the other dimensions [22]. The cure cycle consisted of a constant temperature of 80°C for 30 minutes at the part-mould interface. Figure 4 (b) shows the cool down thermal and mechanical boundary conditions during the demoulding phase. The part was assumed to be demoulded at the process temperature and cooled down to room temperature under natural convection ($80 \text{ W}/(\text{m}^2\text{K})$). This assumption simplifies the cool down simulation with no tool interaction. Uniform degree of cure across the sample width was assumed with the average results of the filling simulation. The simulations were conducted for a cross section of the part in 2D plane strain conditions. Interaction between the mould and the part was defined with a friction coefficient of 0.15 [23], and hard contact normal behaviour. C3D20 quadratic hexahedral elements were used for the moulds and the part. The mesh consisted of 1120 elements for the part and 480 elements for each mould.

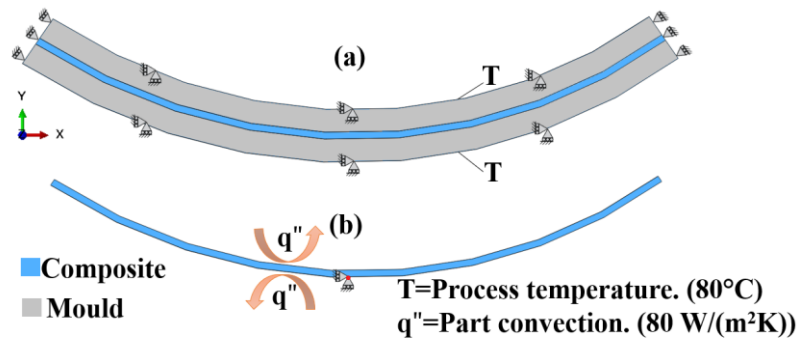


Figure 4: Abaqus-COMPRO boundary conditions for: (a) Curing phase, (b) Demoulding phase.

The degree of cure results from the filling simulations were assumed to be the initial degree of cure for the stress-deformation simulations. The deformation was defined as the spring-in deviation of the part from the intended geometry. Figure 5 shows the spring-in behaviour of the composite after curing and cool down for reference case A. The part geometrical deviation is measured as the distance separation of the manufactured part with the intended geometry.

Figure 6 shows the geometrical deviation results for the cases defined in Table 2. There is a consistent relation between the maximum degree of cure difference in the part after injection and the final deformation of the part. The part geometrical deviation decreases with an increase of maximum degree of cure difference in the part after injection. This finding challenges the previous work on the analysis of the influence of degree of cure gradients for curved geometries. It has been shown that the deformation of the part is augmented as the maximum degree of cure difference increases using a CHILE model for elastic modulus [3]. In the next section, experimental work is presented to investigate and compare the results obtained from the numerical simulations. The purpose of this experimental work is

to validate the accuracy of the simulation results and to provide a more complete understanding of the composite processing with highly reactive thermosets.

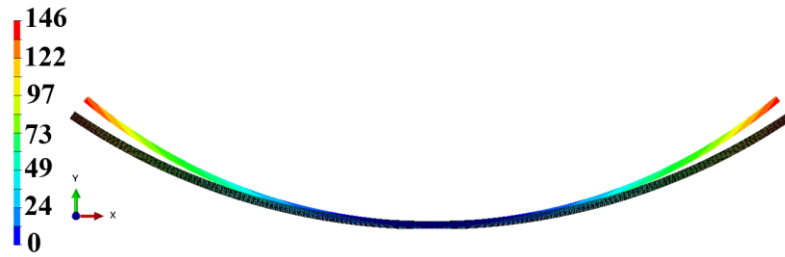


Figure 5: Simulation results of part geometrical deviation for Case A. Units in μm .

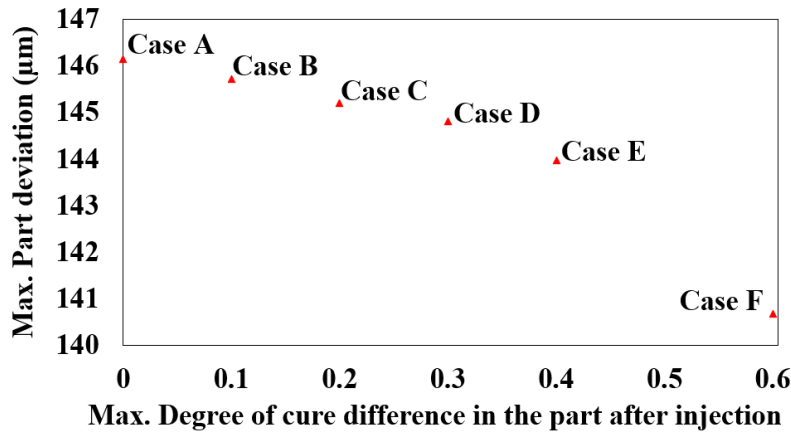


Figure 6: Simulation results of part geometrical deviation for the simulation cases.

4 EXPERIMENTAL VALIDATION

An experimental setup was used for the manufacturing of the representative geometry defined in Figure 2. Figure 7 (a) shows the schematic design of the mould. The mould was CNC machined from a block of aluminum 6060. The setup has four K type thermocouples to record the mould temperature. Five additional K type mould surface thermocouples were used to monitor resin temperature as it flows into the mould. The thermocouples were grounded to ensure high sensitivity and fast data acquisition. Mushroom shaped seals were installed outside the perimeter part to create a tight seal and prevent resin leakage. Resin was injected through a 3.175 mm inner diameter tube from one side and vacuum was applied through the opposite side with a tube with the same characteristics. The mould was installed into a Wabash Genesis press as shown in Figure 7 (b). Cases A, B, C, and D were manufactured under the same process conditions as the simulations. It was found that cases E and F did not reach full impregnation experimentally. Peel 2-S 3D scanner was used to measure the part final geometry. This scanner has an accuracy of up to 0.1 mm. The manufactured parts were coated with SKD-2 solvent-based powder from Magnaflux, and reference points were added for the 3D scanning process, as shown in Figure 8. The scanned surface was imported into Solid Works software and compared with the intended geometry. The experimental part geometrical deviation results are shown in Figure 9. Points were taken on the center line of the part along the length of the part. Figure 9 shows, in black, the path of the points taken. Figure 10 shows the experimental points compared with the fitted quadratic function. The length is normalized from 0 at the injection side and 1 at the vacuum side. The results from simulations are also compared with the experimental points. The points observed in the data represent the waves of the surface created by the separation of the fibre tows on the no-crimp fabric. In order to obtain a representative deformation of the data points, a second order function was used to fit the data. By using this approach, it is possible to obtain a smooth curve that represents the overall trend in the data to quantify the extent of the geometrical deviation. This is an effective method for comparing the experimental part geometrical deviation to the simulation results.

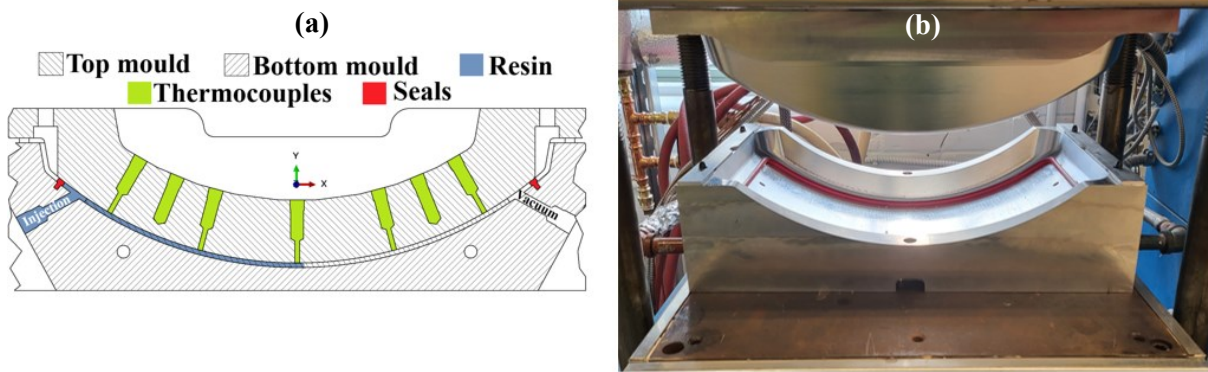


Figure 7: (a) Schematic design of the mould. (b) Physical mould mounted on the Wabash press.



Figure 8: Manufactured experimental parts coated with SKD-2 solvent-based powder.

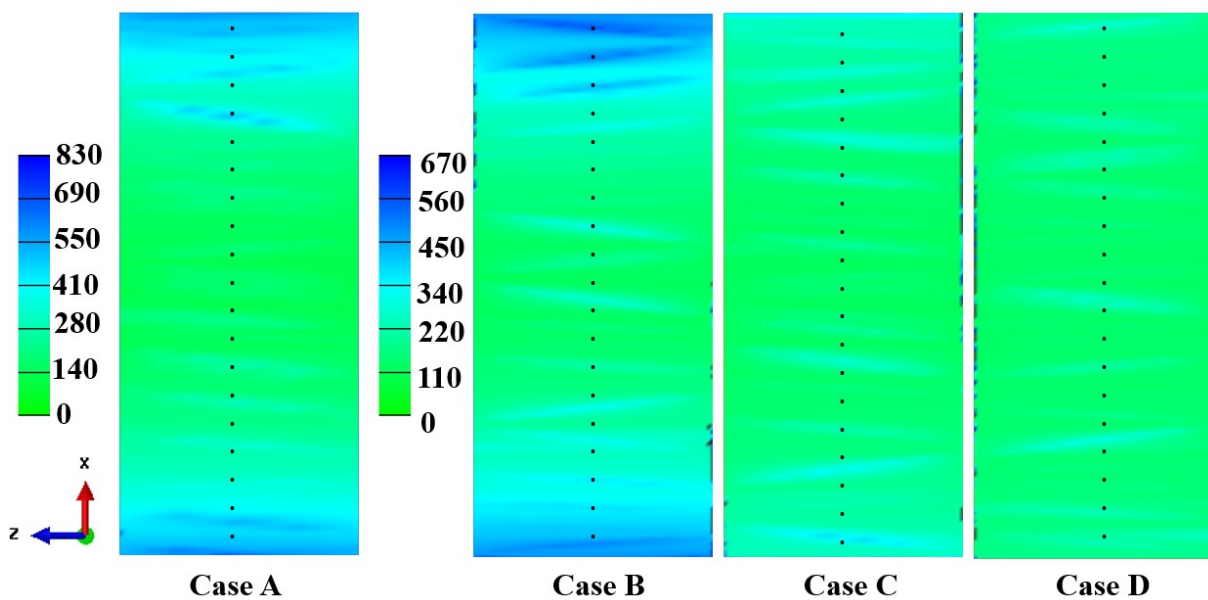


Figure 9: Final part geometrical deviation results from the experimental parts. Units in μm .

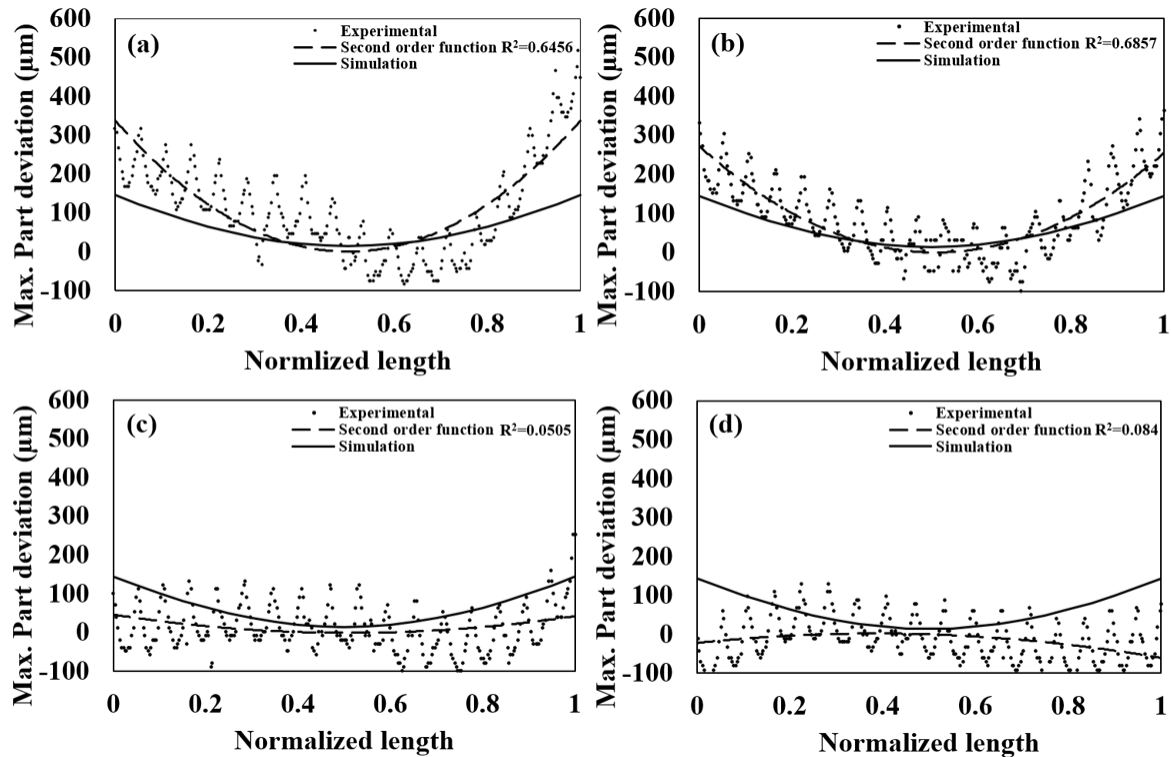


Figure 10: Final part geometrical deviation results from the experimental parts compared with the simulations.
 (a) Case A. (b) Case B. (c) Case C. (d) Case D.

Based on the experimental results, it has been observed that there is a similar trend in the maximal part geometrical deviation in the case with a uniform degree of cure compared to the case with maximal degree of cure difference after the injection step. This is consistent with the previous numerical simulations. The experimental results thus confirm the validity of the numerical simulations and support the notion that minimizing the degree of cure difference after the injection step can result in a reduction in part geometrical deviation. These findings are of significant importance in the liquid moulding processes, as they provide insights into optimizing the process parameters to achieve the desired final shape of the composite part. Overall, the experimental results serve to enhance our understanding of the injection process and provide valuable information for improving the process in practical applications.

4 DISCUSSION

The experiments in this study confirm the tendency of part geometrical deviation, but there is a significant discrepancy between the experimental results and the simulation predictions. Specifically, the simulations predict a maximal deformation difference of only 1.3 μm between cases A and D, while the experiments show a much larger maximal deformation difference of 340 μm between these cases. This discrepancy highlights the challenges of accurately predicting and modelling the complex behaviour of highly reactive thermosets used for liquid moulding processes. The discrepancy between the simulation predictions and experimental results in this study may be attributed, in part, to the assumption that shrinkage only occurs after gelation. This assumption is often made in material models, as this simplifies the characterization labor and the use of more sophisticated equipment [24]. However, in reality, the shrinkage can be complex and may occur at multiple stages throughout the injection and curing processes. In order to improve the accuracy of the simulation and better predict the behaviour of the composite materials, it may be necessary to incorporate more detailed and accurate model of the shrinkage behaviour.

The simplified two-dimensional model used in this study is another factor that may contribute to the discrepancies between the simulation predictions and the experimental results. While two-dimensional models are often used in simulation studies due to their simplicity and computational efficiency, they may not fully capture the complex three-dimensional behaviour of the highly reactive thermosets when processing with liquid moulding. In particular, the two-dimensional model may not fully account for the effects of fibre orientation, in-plane shrinkage and CTE that can significantly influence the behaviour of the composite material during processing.

The results of this study have important implications for the design and processing of composite materials. Specifically, the finding that the degree of cure differences can improve the final shape of the part by counteracting the stresses generated during the processing of composite materials is valuable knowledge that can be used to optimize the design and manufacturing process. This can be particularly useful in the early stages of the mould design process, where injection ports can be strategically placed to minimize the generation of manufacturing stresses and optimize the final shape of the part. However, it is also important to note that the effect of the degree of cure differences may be more complex in some cases, particularly in situations where the degree of cure differences contribute to the generation of residual stresses. In such cases, the degree of cure differences may actually aggravate the deformations and compromise the final shape of the part.

6 CONCLUSION

In conclusion, this study provides valuable insights into the effect of the degree of cure differences on the final shape of composite materials during processing. The experimental and simulation results show that the degree of cure differences can have a significant impact on the final shape of the part, and that this effect should be carefully considered in the design and processing of composite materials. Specifically, the results suggest that the degree of cure differences can counteract the stresses generated during the processing of composite materials, and that this knowledge can be used to optimize the mould design and process parameters to improve the final shape of the part. Overall, this study provides important insights into the behaviour of highly reactive thermosets during processing and highlights the need for continued research in this area to improve the quality, reliability, and performance of composite materials when using these highly reactive thermosets in large scale production.

ACKNOWLEDGMENTS

The authors gratefully acknowledge the financial support provided by the Natural Sciences and Engineering Research Council of Canada (NSERC), PRIMA Quebec, Texonic Inc and IND Experts. The authors would like to thank the technical advice to Lolei Khoun, Paul Trudeau and Nicolas Milliken from the National Research Council of Canada. Special thanks to Anthony Floyd and Alireza Forghani from Convergent Manufacturing. Acknowledgments to the McGill Structures and Composite Materials Laboratory members, specially to our research assistant Lucie Riffard.

REFERENCES

- [1] L. Khoun and P. Trudeau, SNAP RTM: A cost-effective compression-RTM variant to manufacture composite component for transportation applications, *Automotive composites conference and exhibition, Novi, MI, USA, 2018*.
- [2] S. Sarojini, L. Barcenas, L. Khoun and P. Hubert, Simulation and validation of 3D compression resin transfer moulding, *Canadian International Conference on Composite Materials, Fredericton, Canada, 2022*.
- [3] L. Barcenas and P. Hubert, Residual stresses induced by highly reactive thermosets during heated RTM, *Canadian International Conference on Composite Materials, Fredericton, Canada, 2022*.
- [4] P. Prasatya, G. B. McKenna and S. L. Simon, A viscoelastic Model for predicting isotropic residual stresses in thermosetting materials: Effects of processing parameters, *Journal of composite materials*, **Vol. 35**, No. 10/2001, pp. 826-848 (doi: 10.1106/D0JJ-V6Q1-891M-3GJR).

- [5] B.D. Agarwal, L.J. Broutman and K. Chandrashekhara, *Analysis and performance of fiber composites*, 3rd edition, Wiley, 2006.
- [6] A.K. Kaw, *Mechanics of composite materials*, 2nd edition, CRC Press, 2005.
- [7] M. Kinsella, D. Murray, D. Crane, J. Mancinelli and M. Kranjc, Mechanical properties of polymeric composites reinforced with high strength glass fibers, *33rd International SAMPE technical conference, Seattle, WA, USA, 2001*.
- [8] F.T. Wallenberger, J.C. Watson and H. Li, Glass fibers, *ASM International Composites Handbook*. Vol. 21, 2001.
- [9] <http://www.azom.com/properties.aspx?ArticleID=764>. Retrieved on May 5th, 2023.
- [10] M.R. Kamal, Thermoset characterization for moldability analysis, *Polymer engineering and science*, Vol. 14, No. 3, pp 231-239, 1974 (doi:10.1002/pen.760140312).
- [11] A.T. DiBenedetto, Prediction of the glass transition temperature of polymers: A model based on the principle of corresponding states, *Journal of polymer science part B: polymer physics*, Vol. 25, No. 9, pp 1949-1969, 1987 (doi:10.1002/polb.1987.090250914).
- [12] A.A. Johnston, An integrated model of the development of process-induced deformation in autoclave processing of composite structures, *University of British Columbia, Metals and Materials Engineering*, Ph.D. Thesis, 1997.
- [13] A. K. Kaw, *Mechanics of composite materials*, 2nd ed. 2006: CRC press - Taylor & Francis.
- [14] R. J. Thorpe, Experimental Characterization of the Viscoelastic Behavior of a Curing Epoxy Matrix Composite from Pre-Gelation to Full Cure, Master of Applied Science Thesis, The University of British Columbia, (2013).
- [15] J. de Vreugd, K. M. B. Jansen, L. J. Ernst and C. Bohm, Prediction of cure induced warpage of micro-electronic products, *Microelectronics Reliability*, Vol 50, pp. 910-916, 2010, (doi: 10.1016/j.microrel.2010.02.028).
- [16] E. Ruiz and F. Trochu, Thermomechanical Properties during Cure of Glass-Polyester RTM Composites: Elastic and Viscoelastic Modeling, *Journal of Composite Materials*, Vol. 39, No. 10, pp. 881-916, 2005, (doi: 10.1177/0021998305048732).
- [17] D. J. O'Brien, P. T. Mather and S. R. White, Viscoelastic Properties of an Epoxy Resin during Cure, *Journal of Composite Materials*, Vol. 35, No. 10, pp. 883-904, 2001, (doi:10.1177/a037323).
- [18] S. L. Simon, G. B. McKenna and O. Sindt, Modeling the Evolution of the Dynamic Mechanical Properties of a Commercial Epoxy During Cure after Gelation, *Journal of Applied Polymer Science* Vol. 76, pp. 495-508, 2000, (doi:10.1002/(SICI)1097-4628(20000425)76:4<495::AID-APP7>3.0.CO;2-B).
- [19] S. R. White, and Y. K. Kim, Process Induced Residual Stress Analysis of AS4/3501-6, *Composite Material. Mechanics of Composite Structures*, Vol 5, pp. 153-186, 1998, (doi: 10.1080/10759419808945897)
- [20] Y. K. Kim and S. R. White, Stress Relaxation Behavior of 3501-6 Epoxy Resin During Cure, *Polymer Engineering and Science*, Vol. 36, No. 23, pp. 2852-2862, 1996, (doi:10.1002/pen.10686).
- [21] H. F. Brinson, Mechanical and Optical Viscoelastic Characterization of Hysol 4290, *SESA Experimental Mechanics*, Vol 8, pp. 561-566, 1968, (doi:10.1007/BF02327519)
- [22] M. V. Brusckke and S. G. Advani, A numerical approach to model non-isothermal viscous flow through fibrous media with free surfaces, *International Journal for numerical methods in fluids*, Vol. 19, pp 575-603, 1994, (doi:10.1002/flid.1650190704).
- [23] G. Twigg, A. Poursartip and G. Fernlund, An experimental method for quantifying tool-part shear interaction during composites processing, *Composites science and technology*, Vol. 63, pp 1985-2002, 2003, (doi:10.1016/S0266-3538(03)00172-6).
- [24] M. Haider, P. Hubert and L. Lessard, Cure shrinkage characterization and modeling of a polyester resin containing low profile additives, *Composites Part A*, Vol 38, pp 994-1009, 2007, (doi:10.1016/j.compositesa.2006.06.020).